arXiv:cond-mat/0009369v1 [cond-mat.mes-hall] 24 Sep 2000

Kinetics of exciton photoluminescence in type-II semiconductor superlattices

L. S. Braginsky*, M. Yu. Zaharov, A. M. Gilinsky, V. V. Preobrazhenskii, M. A. Putyato, and K. S. Zhuravlev
Institute of Semiconductor Physics, 630090, Novosibirsk, Russia

(February 1, 2008)

Abstract

The exciton decay rate at a rough interface in type-II semiconductor superlattices is investigated. It is shown that the possibility of recombination of indirect excitons at a plane interface essentially affects kinetics of the exciton photoluminescence at a rough interface. This happens because of strong correlation between the exciton recombination at the plane interface and at the roughness. Expressions that relate the parameters of the luminescence kinetics with statistical characteristics of the rough interface are obtained. The mean height and length of roughnesses in GaAs/AlAs superlattices are estimated from the experimental data.

78.66.Fd

Typeset using REVTEX

---

*Electronic address: brag@isp.nsc.ru

I. INTRODUCTION

GaAs/AlAs type-II superlattices are the subject of extensive investigations in the recent decade. Electrons and holes are separated in these structures: holes are confined in the Γ valley of GaAs, whereas electrons are in X valleys of AlAs. Changing the width of AlAs layer during the growth of the structure, it is possible to confine the electrons either in the X_z valley (X valley that is directed along the structure axis [001]) or in the X_{xy} valley (X valley that is directed along the GaAs/AlAs interface: [100] or [010]). The excitons in such structures are indirect in both real and momentum spaces.

Kinetics of the exciton luminescence is investigated by the time-resolved method. The theory by Klein *et al.* [1] is usually used to explain the results of such experiments. The theory has been developed to consider the no-phonon radiative decay rates of indirect excitons in alloy semiconductors (e.g., $\mathrm{Ga}_{1-x}\mathrm{Al}_x\mathrm{As}$). The recombination of indirect excitons occurs because of intervalley scattering of electrons at the potential fluctuations caused by the compositional disorder. These short-range scatterers are necessary to compensate the large momentum of the electron in the X valley. The nonexponential dependence of the decay rate has been obtained

$$I(t) \propto e^{-w_0 t}(1 + 2w_r t)^{-3/2}. \tag{1}$$

Where the value w_r is connected with the compositional disorder. The exponential factor has been included in Eq. (1) to consider different nonstochastic processes of the exciton recombination (e.g., the phonon-assisted recombination). This is possible only in the absence of correlation between stochastic and nonstochastic processes.

The possibility to apply the theory[1] for superlattices has been discussed by F. Minami *et al.*.[2] Authors suppose the short-range scatterers are distributed along the plane boundary. This assumption justifies the application of Eq. (1) for superlattices; however, it does not allow to relate the parameter w_r with characteristics of the rough interface, e.g., the mean height and length of roughnesses. I. Krivorotov *et al.*[3] have showed that nonradiative decay due to exciton trapping by interfacial defects also results in nonexponential factor in Eq. (1). Nevertheless, Eq. (1), wherein the parameters w_r and w_0 are considered as trial, is commonly used for explanation of the experimental results.[4]

It should be noted that roughnesses are not necessary for the recombination of X_z excitons. Their recombination occurs even at a plain interface where the normal component of the electron momentum relaxes. This important point also distinguishes the exciton recombination in superlattices. The process, however, can not be taken into account by a simple exponential factor. Indeed, the wave function of the electron at a rough interface is the sum of its regular and diffuse components. The first one exists at a plane interface, whereas the latter is due to the roughnesses. For this reason the crossed terms arise in the interband matrix element; so that the probability of the exciton recombination, which is determined by the squared module of this matrix element, is no longer a simple sum of the probabilities of the recombination at the plane interface and at the roughnesses. This correlation leads to a more complicated relation than the simple exponential factor in Eq. (1).

In this paper we consider a more realistic model of the rough interface. We show that Eq. (1) holds for the decay rate of X_{xy} excitons and relate the w_r value with parameters of the rough interface. We determine the decay rate of X_z excitons. In particular, it is found that this value at large times behaves roughly as $I(t) \propto \exp(-w_0 t)/t$, rather than $I(t) \propto \exp(-w_0 t)/t^{3/2}$ as it is predicted by Eq. (1).

Our experiments on the GaAs/AlAs type-II superlattices confirm these results. We use the experimental data for the radiative decay rates to estimate the parameters of the rough interface. The mean height of roughnesses was found to be close to the lattice constant, whereas their mean length is about $50\,\mathring{A}$.

II. RADIATIVE DECAY RATES OF INDIRECT EXCITONS IN SUPERLATTICES. THEORY

Let $z = 0$ be the interface between GaAs ($-d_1 < z < 0$) and AlAs ($0 < z < d_2$), and $\boldsymbol{\rho}$ be the vector in the XY plane. We consider the exiton recombination at the interface and write the exciton wave function as follows:[5]

$$\phi(\mathbf{r}_e, \mathbf{r}_h) = f_e(z_e) f_h(z_h) G(\boldsymbol{\rho}_e - \boldsymbol{\rho}_h, z_e, z_h).$$

Where $\mathbf{r}_e = \{\boldsymbol{\rho}_e,\ z_e\}$ and $\mathbf{r}_h = \{\boldsymbol{\rho}_h,\ z_h\}$ are coordinates of the electron and the hole, $f_e(z_e)$ and $f_h(z_h)$ are their wave functions in the absence of Coulomb interaction; the function G takes into account this interaction. The probability for the exciton recombination is proportional to $G^2(\mathbf{0})$ $[G(\mathbf{0}) \equiv G(\boldsymbol{\rho}_e = \boldsymbol{\rho}_h, z_e = z_h = 0)]$ and the squared module of the matrix element

$$\mathcal{P} = \int f_e(z) \boldsymbol{\nabla} f_h(z)\, dz\, d^2\boldsymbol{\rho}. \tag{2}$$

The functions $f_e(z_e)$ and $f_h(z_h)$ can be expressed via envelope wave functions of the electron and the hole in the conduction and valence bands of GaAs and AlAs. To determine the envelopes, the appropriate boundary conditions at the GaAs/AlAs interface should be imposed. The roughness of the interface has an influence on these boundary conditions and, therefore, affects the envelopes. We shall consider the rough interface where the mean height of roughnesses is small in comparison with the electron wavelength (or the exciton size). This allows us to use the boundary conditions at the rough interface[6] to consider an influence of roughnesses on the exciton recombination.

A. Boundary conditions for the envelope wave functions at a GaAs/AlAs interface

1. Boundary conditions at a plane interface

In general, the boundary conditions for the electron envelopes can be written as follows:

$$\begin{pmatrix} \Psi^r_\Gamma \\ \Psi^{r'}_\Gamma \\ \Psi^r_{Xxy} \\ \Psi^{r'}_{Xxy} \\ \Psi^r_{Xz} \\ \Psi^{r'}_{Xz} \end{pmatrix} = \tilde{T} \begin{pmatrix} \Psi^l_\Gamma \\ \Psi^{l'}_\Gamma \\ \Psi^l_{Xxy} \\ \Psi^{l'}_{Xxy} \\ \Psi^l_{Xz} \\ \Psi^{l'}_{Xz} \end{pmatrix}. \tag{3}$$

Where $\Psi^{l,r}_{\Gamma,Xxy,Xz}$ are the envelopes which correspond to the Γ, X_{xy}, and X_z valleys of GaAs and AlAs; $\Psi^{l,r'}_{\Gamma,Xxy,Xz} \equiv \partial\Psi^{l,r}_{\Gamma,Xxy,Xz}/\partial z$ are their normal derivatives. The elements $\tilde{t}_{ik}$ of the 6×6 matrix $\tilde{T}$ are determined by the interface structure. They are independent of the electron energy. For the GaAs/AlGaAs interface they have been calculated by Ando *et al.*.[7]

We shall consider the particular cases of X_z and X_{xy} excitons. This allows us to simplify Eq. (3). First, we omit mixing between X_z and X_{xy} valleys. Second, the energy position of Γ minimum in AlAs is considerably higher than that of X minimum. For this reason the wave function Ψ^r_Γ decays rapidly apart of the interface. We have $\Psi^r_\Gamma \propto \exp(-\gamma^r z)$, $\Psi^{r'}_\Gamma = -\gamma^r \Psi^r_\Gamma$, where $\gamma^r = \sqrt{2m^r_\Gamma(E_\Gamma - \varepsilon_e)}$ (here m^r_Γ is effective mass in the Γ valley of AlAs, $\varepsilon_e \approx E_X$ is the electron energy, E_Γ and E_X are energies of bottoms of the Γ and X valleys) can be considered as independent of the electron energy. By eliminating of Ψ^r_Γ from Eq. (3), for X_z electrons we find:

$$\begin{cases} \Psi^r_{Xz} = \Psi^l_{Xz}, \\ \Psi^{r'}_{Xz} = t^z_{41}\Psi^l_\Gamma + t^z_{44}\Psi^{l'}_{Xz}, \\ \Psi^l_\Gamma + t^z_{12}\Psi^{l'}_\Gamma + t^z_{13}\Psi^l_{Xz} = 0. \end{cases} \tag{4a}$$

Where $t^z_{44} \approx m^r_{Xl}/m^l_{Xl} \approx 1$, this value takes into account the difference of longitudinal effective masses in the X valleys of AlAs and GaAs; $t^z_{41} = t_{\Gamma X} m^r_{Xl}/(m_e a)$, $t^z_{12} = m^r_\Gamma/(m^l_\Gamma \gamma^r)$, $t^z_{13} = t_{\Gamma X} m^l_\Gamma/(m_e a \gamma^r) \ll 1$; $t_{\Gamma X} \approx 1$ is the parameter of Γ–X mixing. Other elements of the t^z_{ik} matrix are small; this is the result of numerical calculations.[7]

Note that the band states in the X valley result from interaction of two close-lying bands: lower X_1 and upper X_3; meanwhile only the X_3 states mix effectively with Γ states. This means that $t_{\Gamma X} \approx 1$ is the upper estimation of Γ–X mixing.

It is sufficient to consider only X valleys of each contacted material when X_{xy} electrons are investigated. Assuming $\Psi^{l'}_\Gamma = \gamma^l \Psi^l_\Gamma$, where $\gamma^l \sim 2\pi/a$ (a is the lattice constant), from Eq. (3) we find:

$$\begin{aligned} \Psi^r_{Xxy} &= t^{xy}_{11}\Psi^l_{Xxy} + t^{xy}_{12}\Psi^{l'}_{Xxy}, \\ \Psi^{r'}_{Xxy} &= t^{xy}_{21}\Psi^l_{Xxy} + t^{xy}_{22}\Psi^{l'}_{Xxy}. \end{aligned} \tag{4b}$$

Where $|t^{xy}_{12}| \ll 1$, $|t^{xy}_{21}| \ll a^{-1}$, $|t^{xy}_{11}| \approx 1$, and $t^{xy}_{22} \approx m^r_{Xt}/m^l_{Xt} \approx 1$; m^r_{Xt} and m^l_{Xt} are the transversal effective masses of AlAs and GaAs.

The bands of the light and heavy holes are splitted due to the size quantization. This allows us to consider only the heavy holes in each material and write the boundary conditions for them as follows:

$$\begin{aligned} \Psi^r_h &= t^h_{11}\Psi^l_h + t^h_{12}\Psi^{l'}_h, \\ \Psi^{r'}_h &= t^h_{21}\Psi^l_h + t^h_{22}\Psi^{l'}_h. \end{aligned} \tag{4c}$$

Where $\Psi^{l,r}_h$ are the envelopes for the heavy holes in each material.

2. Boundary conditions at a rough interface

We shall consider the model of a rough interface that is presented on Fig. 1. This model is in agreement with optical[8] and structural[9] investigations of GaAs/AlAs interface. The interface looks like an array of the plane areas of the same crystallographic orientation. The random function $z = \xi(\boldsymbol{\rho})$ of the coordinates in the XY plane determines the positions of these areas relative to $z = 0$.

We assume the average height of roughnesses h to be small in comparison with the electron wavelength. Then it is possible to describe the rough interface by means of the correlation function $W(\boldsymbol{\rho'}, \boldsymbol{\rho''}) = \overline{\xi(\boldsymbol{\rho'})\xi(\boldsymbol{\rho''})}$. For the homogeneous rough interface $W(\boldsymbol{\rho'}, \boldsymbol{\rho''}) = W(\boldsymbol{\rho'} - \boldsymbol{\rho''})$, i.e., the correlation function is the function of one variable: $\boldsymbol{\rho} = \boldsymbol{\rho'} - \boldsymbol{\rho''}$. There are two parameters that are most important when the statistical properties of a rough interface are considered: $h^2 = W(0)$ and the correlation length l — the mean attenuation length of the correlation function. In our model the correlation length l can be associated with the mean size of the plane area.

The special form of the rough interface (Fig. 1) allows us to apply the boundary conditions (4), which are applicable at a plane interface, at each plane $z = \xi$. The inequality $|\xi\Psi'| \sim h/\lambda \ll 1$ (λ is the electron wavelength) allows to rewrite these boundary conditions at a plane $z = 0$. After some algebra we obtain:

$$\begin{aligned}
&\Psi^r_{Xz} = -t^z_{41}\eta(\xi)\xi(\boldsymbol{\rho})\Psi^l_\Gamma + \Psi^l_{Xz} + (1 - t^z_{44})\xi(\boldsymbol{\rho})\Psi^{l'}_{Xz},\\
&\Psi^{r'}_{Xz} = t^z_{41}\eta(\xi)\Psi^l_\Gamma + t^z_{41}\eta(\xi)\xi(\boldsymbol{\rho})\Psi^{l'}_\Gamma t^z_{44}\Psi^{l'}_{Xz},\\
&\Psi^l_\Gamma + [t^z_{12} + \xi(\boldsymbol{\rho})]\Psi^{l'}_\Gamma + t^z_{13}\eta^*(\xi)\Psi^l_{Xz} + t^z_{13}\eta^*(\xi)\xi(\boldsymbol{\rho})\Psi^{l'}_{Xz},
\end{aligned} \tag{5a}$$

for electrons in the X_z valley;

$$\begin{aligned}
&\Psi^r_{Xxy} = \Psi^l_{Xxy} + (1 - t^{xy}_{22})\xi(\boldsymbol{\rho})\Psi^{l'}_{Xxy},\\
&\Psi^{r'}_{Xxy} = t^{xy}_{21}\Psi_{Xxy} + t^{xy}_{22}\Psi^{l'}_{Xxy},
\end{aligned} \tag{5b}$$

for electrons in the X_{xy} valley; and

$$\begin{aligned}
&\Psi^r_h = \Psi^l_h + (1 - t^h_{22})\xi(\boldsymbol{\rho})\Psi^{l'}_h,\\
&\Psi^{r'}_h = t^h_{21}\Psi_h + t^h_{22}\Psi^{l'}_h,
\end{aligned} \tag{5c}$$

for the holes. Factor $\eta(\xi) = \exp(2\pi i\xi/a)$ in Eq. (5a) takes the two values ± 1 for $\xi = a$ or $\xi = a/2$. It has been introduced in Ref.[10] to take into account the symmetry properies of the Bloch functions with respect to translation by a single monomolecular layer ($a/2$) along the z axis. The Bloch function of the electron in the X_z valley changes its sigh under this translation whereas the Bloch function of the electron in the Γ valley does not. Therefore, the parameter $t_{\Gamma X}$ of Γ–X mixing also should change sigh under such translation. This is not important at a plane interface, but it must be taken into account when the relative positions of some interfaces are considered. We assume $|t^{xy,h}_{21}| \ll a^{-1}$: this is the result of numerical calculations.[7]

Unlike Eqs. (4) the boundary conditions (5) contain the terms depended on ξ. They would not be important, if $\xi = \text{const}$. Then they relevant to the phase shift of the wave functions due to the shift of the interface. However, these terms become important when ξ depends on $\boldsymbol{\rho}$. Interference of the electrons scattered from the neighboring planes in the vicinity of steps (like point 1 on Fig. 1) results in the diffuse component of their wave function. The mean size of the region at the step where the interference occurs is the parallel-to-interface component of the electron wavelength. Hence the ratio of this size to the size of the plane area l characterizes the roughnesses influence on the electrons.

We separate the diffuse components $\varphi^{l,r}_{\Gamma,X_z,X_{xy}}$ of the envelope wave functions and write the envelopes as follows:[11]

$$\begin{aligned}&\Psi^{l,r}_{\Gamma,X_z,X_{xy}} = \Phi^{l,r}_{\Gamma,X_z,X_{xy}} + \varphi^{l,r}_{\Gamma,X_z,X_{xy}}, \\ &\text{where} \quad \overline{\varphi^{l,r}_{\Gamma,X_z,X_{xy}}} = 0.\end{aligned} \tag{6}$$

Using the boundary conditions (5), for the envelopes $\Phi^{l,r}_{\Gamma,X_z,X_{xy}}$ and $\varphi^{l,r}_{\Gamma,X_z,X_{xy}}$ (see Ref.[6] for the details) we obtain

$$\Phi^l_\Gamma(\mathbf{r}) = T_\Gamma e^{-ip_\Gamma z}, \quad \Phi^l_{X_z,X_{xy}}(\mathbf{r}) = T_{X_z,X_{xy}} e^{\gamma_{X_z,X_{xy}} z}, \quad \Phi^r_{X_z,X_{xy}}(\mathbf{r}) = e^{-iqz} + R_{X_z,X_{xy}} e^{iqz},$$

$$\Phi^l_h(\mathbf{r}) = e^{ipz} + R_h e^{-ipz}, \quad \Phi^r_h(\mathbf{r}) = T_h e^{-\gamma_h z},$$

$$\begin{aligned}
\varphi^l_\Gamma(\mathbf{r}) &= \frac{2q}{(2\pi)^2}\int_{-\infty}^{\infty} A^l_\Gamma(\boldsymbol{k}_\parallel)\tilde{\xi}(\boldsymbol{k}_\parallel)e^{i(\boldsymbol{k}_\parallel\boldsymbol{\rho} - k_\Gamma z)}\,d\boldsymbol{k}_\parallel,\\
\varphi^l_{X_z,X_{xy}}(\mathbf{r}) &= \frac{2q}{(2\pi)^2}\int_{-\infty}^{\infty} A^l_{X_z,X_{xy}}(\boldsymbol{k}_\parallel)\tilde{\xi}(\boldsymbol{k}_\parallel)e^{i\boldsymbol{k}_\parallel\boldsymbol{\rho} + \text{\ae}_{\Gamma,X_z,X_{xy}} z}\,d\boldsymbol{k}_\parallel,\\
\varphi^r_{X_z,X_{xy}}(\mathbf{r}) &= \frac{2q}{(2\pi)^2}\int_{-\infty}^{\infty} A^r_{\Gamma,X_z,X_{xy}}(\boldsymbol{k}_\parallel)\tilde{\xi}(\boldsymbol{k}_\parallel)e^{i(\boldsymbol{k}_\parallel\boldsymbol{\rho} + k_{X_z,X_{xy}} z)}\,d\boldsymbol{k}_\parallel,\\
\varphi^l_h(\mathbf{r}) &= \frac{2p}{(2\pi)^2}\int_{-\infty}^{\infty} A^l_h(\boldsymbol{k}_\parallel)\tilde{\xi}(\boldsymbol{k}_\parallel)e^{i(\boldsymbol{k}_\parallel\boldsymbol{\rho} - k_h z)}\,d\boldsymbol{k}_\parallel,\\
\varphi^r_h(\mathbf{r}) &= \frac{2p}{(2\pi)^2}\int_{-\infty}^{\infty} A^r_h(\boldsymbol{k}_\parallel)\tilde{\xi}(\boldsymbol{k}_\parallel)e^{i\boldsymbol{k}_\parallel\boldsymbol{\rho} - \text{\ae}_h z}\,d\boldsymbol{k}_\parallel.
\end{aligned} \tag{7}$$

Where

$$\begin{aligned}
&k_\Gamma(\boldsymbol{k}_\parallel) = \sqrt{2m_\Gamma(\varepsilon_e - E^l_\Gamma) - {\boldsymbol{k}_\parallel}^2}, \quad \text{\ae}_{X_z}(\boldsymbol{k}_\parallel) = \sqrt{2m^l_{Xl}(E^l_{X_z} - \varepsilon_e) + {\boldsymbol{k}_\parallel}^2},\\
&\text{\ae}_{X_{xy}}(\boldsymbol{k}_\parallel) = \sqrt{2m^l_{Xt}(E^l_{X_{xy}} - \varepsilon_e) + {\boldsymbol{k}_\parallel}^2}, \quad k_{X_z}(\boldsymbol{k}_\parallel) = \sqrt{2m^r_{Xl}(\varepsilon_e - E^r_{X_z}) - {\boldsymbol{k}_\parallel}^2},\\
&k_{X_{xy}}(\boldsymbol{k}_\parallel) = \sqrt{2m^r_{Xt}(\varepsilon_e - E^r_{X_{xy}}) - {\boldsymbol{k}_\parallel}^2}, \quad k_h(\boldsymbol{k}_\parallel) = \sqrt{2m^l_h(E^l_h - \varepsilon_h) - {\boldsymbol{k}_\parallel}^2},\\
&\text{\ae}_h(\boldsymbol{k}_\parallel) = \sqrt{2m^r_h(\varepsilon_h - E^r_h) + {\boldsymbol{k}_\parallel}^2}, \quad \operatorname{Im} k_{X_z,X_{xy},h} \geq 0,\\
&T_\Gamma = \frac{2iqt^z_{13}\eta(\xi)}{t^z_{44}\gamma_{X_z}}, \quad T_{X_z} = -\frac{2iq}{t^z_{44}\gamma_{X_z}}, \quad R_{X_z} = -1 - \frac{2iq}{t^z_{44}\gamma_{X_z}},\\
&T_{X_{xy}} = \frac{2iq}{t^{xy}_{21} + t^{xy}_{22}\gamma_{X_{xy}}}, \quad R_{X_{xy}} = -1 + \frac{2iq}{t^{xy}_{21} + t^{xy}_{22}\gamma_{X_{xy}}},\\
&T_h = -\frac{2ip}{-t^h_{21} + t^h_{22}\gamma_h}, \quad R_h = -1 - \frac{2ip}{-t^h_{21} + t^h_{22}\gamma_h},\\
&A^l_\Gamma = \frac{it^z_{13}\eta(\xi)}{t^z_{44}}, \quad A^r_{X_z} = -\frac{i}{t^z_{44}}\left(\frac{t^z_{13}t^z_{41}}{\gamma_{X_z}} + 1 - t^z_{44}\right), \quad A^l_{X_z} = -\frac{k_{X_z}}{\text{\ae}_{X_z}{t^z_{44}}^2}\left(\frac{t^z_{13}t^z_{41}}{\gamma_{X_z}} + 1 - t^z_{44}\right),\\
&A^r_{X_{xy}} = i\frac{t^{xy}_{22}\text{\ae}_l\text{\ae}_{X_{xy}}(1 - t^{xy}_{22})}{(t^{xy}_{21} + \text{\ae}_{X_{xy}}t^{xy}_{22})(t^{xy}_{22}\text{\ae}_l + ik_{X_{xy}})}, \qquad A^l_{X_{xy}} = k_z\frac{\text{\ae}_{X_{xy}}(1 - t^{xy}_{22})}{(t^{xy}_{21} + \text{\ae}_{X_{xy}}t^{xy}_{22})(t^{xy}_{22}\text{\ae}_l + ik_{X_{xy}})},\\
&A^r_h = -\frac{k_h(1 - t^h_{22})}{t^h_{22}(\text{\ae}_h t^h_{22} - t^h_{21})}, \qquad A^l_h = i\frac{\text{\ae}_h(1 - t^h_{22})}{\text{\ae}_h t^h_{22} - t^h_{21}}.
\end{aligned}$$

Here $\tilde{\xi}(\boldsymbol{k}_{\|}) = \int \xi(\boldsymbol{\rho}) e^{-i\boldsymbol{k}_{\|}\boldsymbol{\rho}}\, d\boldsymbol{\rho}$, $\gamma_{X_z,X_{xy},h} = \ae_{X_z,X_{xy},h}(0)$, $p_\Gamma = k_\Gamma(0)$; E^l_Γ, $E^l_{X_z}$, $E^l_{X_{xy}}$, $E^r_{X_z}$, $E^r_{X_{xy}}$, E^l_h, and E^r_h are energies of extrema of the appropriate bands. Integration in Eq. (7) is carried out over the whole plane because $\xi(\boldsymbol{\rho})$ is not periodical function of $\boldsymbol{\rho}$. The values of normal-to-interface components of the wave vectors of the electrons q and holes p are determined by the boundary conditions at the interfaces: $z = -d_1$ for p and $z = d_2$ for q (where d_1 and d_2 are widths of GaAs and AlAs layers). In general, they depends on the valley under consideration: $\tan\frac{qd_2}{2} = -\frac{q}{\gamma_{X_z}}$ for electrons in the X_z valley, $\tan qd_2 = -\frac{2q}{t^{xy}_{22}\gamma_{X_{xy}} + t^{xy}_{21}}$ for electrons in the X_{xy} valley, and $\tan pd_1 = -\frac{2p}{t^h_{22}\gamma_h - t^h_{21}}$ for the holes. We assume, however, the strong confinement of electrons and holes in the appropriate layers $\gamma_{X_z,X_{xy},h} \gg p, q$, so that $p \approx \pi/d_1$ and $q \approx \pi/d_2$.

The wave function of the electron in the GaAs Γ valley is small, $p_\Gamma \ll p$; nevertheless, it is real. This distinguish the short-period GaAs/AlAs superlattices from other type-II structures, where the electron wave function decays rapidly from the interface. The electron density is large in AlAs and small, but almost constant, in GaAs. This small part of the electron density could be essential for the exiton recombination would the effective parameter of Γ–X mixing t^z_{13} be sufficently large.

B. Radiative decay rates of indirect excitons at a rough interface

To determine the wave functions $f_e(z)$ and $f_h(z)$, we have to insert the corresponding Bloch amplitudes into expressions for the envelopes Ψ_e and Ψ_h (6). For instance, for the X_z exciton at a plane interface, we have

$$f_e(\mathbf{r}) = \frac{1}{\sqrt{N_1}} \begin{cases} T_\Gamma u_\Gamma(\mathbf{r}) e^{\gamma_\Gamma z} \\ \quad + T_{X_z} u_X(\mathbf{r}) e^{\left(\gamma_{X_z} - \frac{2\pi i}{a}\right) z}, & z < 0, \\ \\ u^*_X(\mathbf{r}) e^{i\left(q - \frac{2\pi i}{a}\right) z} \\ \quad + R_{X_z} u_X(\mathbf{r}) e^{-i\left(q - \frac{2\pi i}{a}\right) z}, & z > 0, \end{cases}$$

$$f_h(\mathbf{r}) = \frac{1}{\sqrt{N_2}} \begin{cases} v(\mathbf{r}) e^{ipz} + R_h v^*(\mathbf{r}) e^{-ipz}, & z < 0, \\ T_h v(\mathbf{r}) e^{-\gamma_h z}, & z > 0. \end{cases} \tag{8}$$

Where N_1 and N_2 are numbers of atoms in the AlAs and GaAs layers, $u_\Gamma(\mathbf{r})$, $u_X(\mathbf{r})$ and $v(\mathbf{r})$ are Bloch amplitudes of electrons in the Γ and X valleys, and the holes; we assume these amplitudes to be periodical functions of $\mathbf{r}$.

At a rough interface we have to add also the diffuse components of the wave functions. To do that, we have to multiply $\varphi(\mathbf{r})$ (7) by the corresponding Bloch amplitudes. Usually the mean size of Bloch amplitudes is small in comparison with the lattice constant. This allows us to assume that $\boldsymbol{\nabla}$-operator in Eq. (2) acts only on these amplitudes and to separate the integration of them from integration of the envelopes. Then the matrix element (2) can be written as $\mathcal{P} = \mathcal{P}_1 + \mathcal{P}_2 + \mathcal{P}_3$, where

$$\mathcal{P}_1 = \sum_{\Gamma,X} U_{\Gamma,X} \int \Phi_{\Gamma,X_z,X_{xy}} \Phi_h \, dz\, d\boldsymbol{\rho},$$

$$\mathcal{P}_2 = \sum_{\Gamma,X} U_{\Gamma,X} \int [\Phi_{\Gamma,X_z,X_{xy}} \varphi_h + \Phi_h \varphi_{\Gamma,X_z,X_{xy}}]\, dz\, d\boldsymbol{\rho}, \tag{9}$$

$$\mathcal{P}_3 = \sum_{\Gamma,X} U_{\Gamma,X} \int \varphi_{\Gamma,X_z,X_{xy}} \varphi_h \, dz\, d\boldsymbol{\rho}.$$

Here $\Phi = \Phi^l$, $\varphi = \varphi^l$ if $z < \xi$; $\Phi = \Phi^r$, $\varphi = \varphi^r$ if $z > \xi$; $U_\Gamma = \Omega_0^{-1} \int_{\Omega_0} u_\Gamma(\mathbf{r}) \boldsymbol{\nabla} v(\mathbf{r})\, d\mathbf{r}$, $U_X = \Omega_0^{-1} \int_{\Omega_0} u_X(\mathbf{r}) \boldsymbol{\nabla} v(\mathbf{r})\, d\mathbf{r}$, and Ω_0 is the unit cell.

The rate of the exciton recombination is

$$w = \Lambda \left(|\mathcal{P}_1|^2 + \mathcal{P}_1 \mathcal{P}_2^* + \mathcal{P}_1^* \mathcal{P}_2 + \mathcal{P}_1 \mathcal{P}_3^* + \mathcal{P}_1^* \mathcal{P}_3 + |\mathcal{P}_2|^2 \right),$$

$$\Lambda = \frac{4\hbar e^2 \omega}{3 m_e^2 c^3} G^2(\mathbf{0}). \tag{10}$$

Where $\hbar\omega$ is the exciton energy, e, m_e and c are the fundamental constants.

The luminescence magnitude $I(t)$ is proportional to the recombination rate w and the number of excitons at the time t. We assume this number to be proportional to $\exp(-wt)$ (or $\exp[-(w_0 + w)t]$, if some nonstochastic process with the rate w_0 occurs). The w value is stochastical, since it depends on ξ. Therefore, to determine the luminescence magnitude, we have to average the value of $w \exp(-wt)$ over the realization of the random function ξ. This could be done if we know the distribution $P(w)$ of the w value: $\overline{w \exp(-wt)} = \int_0^\infty w \exp(-wt) P(w)\, dw$. The distribution $P(w)$ essentially depends on $\mathcal{P}_1$, whether or not it vanishes.

If $\mathcal{P}_1 = 0$ (i.e., if the exciton recombination at a plane interface is forbidden) then w is proportional to squared module of $\mathcal{P}_2$. The linear dependence between $\mathcal{P}_2$ and the random variable ξ follows from Eqs. (7) and (9). Therefore, if the distribution of ξ is Gaussian, then the distribution of $\mathcal{P}_2$ is also Gaussian and the distribution of w is exponential. This means applicability of arguments of Refs.[1,2], so that $I(t)$ is determined by Eq. (1) where $w_r = \Lambda |\mathcal{P}_2|^2$. For the case of X_{xy} exciton we have

$$\mathcal{P}_2 = \frac{4pqU_X}{\sqrt{N_1 N_2}} \sum_{\mathbf{g}} \left[\frac{1 - t_{22}^h}{\gamma_{X_{xy}}^2} \tilde{\xi}\left(\mathbf{q}_X + \mathbf{g}\right) \right. \\ \left. + \frac{1 - t_{22}^{xy}}{\gamma_h^2} \tilde{\xi}^* \left(\mathbf{q}_X + \mathbf{g}\right) \right],$$

and

$$w_r = \frac{16\pi^4 a^4 |U_X|^2 \Lambda}{d_1^3 d_2^3} \left[\frac{(1 - t_{22}^h)^2}{\gamma_{X_{xy}}^4} + \frac{(1 - t_{22}^{xy})^2}{\gamma_h^4} \right] \tilde{W}\left(\frac{\pi}{a}\right). \tag{11}$$

Where $\tilde{W}(\mathbf{k}) = \int W(\boldsymbol{\rho}) e^{-ik\rho}\, d^2\boldsymbol{\rho}$ is the Fourier transform of the correlation function; $\mathbf{q}_X = \{2\pi/a, 0, 0\}$ is the wave number of the X valley, $\mathbf{g}$ is a two-dimensional reciprocal lattice vector, it arises here since integration in Eq. (7) has not been restricted by the first Brillouin zone.

If $\mathcal{P}_1 \neq 0$ (i.e., if the exciton recombination at a plane interface is allowed) then the linear with respect to $\mathcal{P}_2$ terms in Eq. (10) are nonzero. This allows to omit the terms with $\mathcal{P}_3$ and $|\mathcal{P}_2|^2$, which are quadratic in ξ, or replace them with their average values. Then w

becomes the linear function of the random variable ξ. If the distribution of ξ is Gaussian then the distribution of w is Gaussian too, i.e.,

$$P(w) = \frac{1}{\sigma\sqrt{2\pi}} e^{-\frac{(w-\overline{w})^2}{2\sigma^2}}.$$

Where $\overline{w} = \Lambda|\mathcal{P}_1|^2$, and $\sigma = \left[\overline{|w-\overline{w}|^2}\right]^{1/2}$.

Hence

$$\begin{aligned} I(t) &= \frac{e^{-w_0 t}}{\sigma\sqrt{2\pi}} \int_0^\infty w e^{-wt-\frac{(w-\overline{w})^2}{2\sigma^2}}\, dw \\ &= e^{-(\overline{w}+w_0)t}\left[\frac{\sigma}{\sqrt{2\pi}} + \frac{\overline{w}-\sigma^2 t}{2} e^{\frac{\sigma^2 t^2}{2}} \operatorname{erfc}\left(\frac{\sigma t}{\sqrt{2}}\right)\right]. \end{aligned} \tag{12}$$

If $|\mathcal{P}_1| \gg |\mathcal{P}_2|$, then $\sigma^2 \simeq 2\Lambda^2|\mathcal{P}_1|^2\overline{\mathcal{P}_2\mathcal{P}_2^*}$. For the case of X_z exciton we have

$$\begin{aligned} \mathcal{P}_1 &= \frac{2a^3}{\sqrt{d_1 d_2}}\left[4\left(\frac{d_1}{d_2}\right)\frac{t_{13}^z}{\gamma_{X_z} t_{44}^z} U_\Gamma + \left(\frac{a}{d_1}\right)\frac{1}{\gamma_h t_{22}^h} U_X\right], \\ \mathcal{P}_2 &= \frac{2a^2}{\sqrt{d_1 d_2}}\left[8\left(\frac{d_1}{d_2}\right)\frac{t_{13}^z}{t_{44}^z} U_\Gamma + \right. \\ &\left. \frac{2\pi i a}{t_{22}^h d_1}\left(\frac{1}{t_{44}^z\gamma_{X_z} d_2} - \frac{1-t_{22}^h}{t_{22}^h\gamma_h d_1}\right) U_X\right]\eta(\xi)\tilde{\xi}(0), \end{aligned} \tag{13}$$

so that

$$\begin{aligned} \overline{w} &= \frac{4\Lambda a^6}{d_1 d_2}\left[4\left(\frac{d_1}{d_2}\right)\frac{t_{13}^z}{\gamma_{X_z} t_{44}^z} U_\Gamma + \left(\frac{a}{d_1}\right)\frac{1}{\gamma_h t_{22}^h} U_X\right]^2, \\ \sigma^2 &= \frac{2\Lambda a^4 \overline{w}}{d_1 d_2}\left[64\left(\frac{d_1}{d_2}\right)^2 \frac{{t_{13}^z}^2}{{t_{44}^z}^2} U_\Gamma^2 + \right. \\ &\left. \left(\frac{2\pi a}{t_{22}^h d_1}\right)^2\left(\frac{1}{t_{44}^z\gamma_{X_z} d_2} - \frac{1-t_{22}^h}{t_{22}^h\gamma_h d_1}\right)^2 U_X^2\right]\tilde{W}(0). \end{aligned} \tag{14}$$

The first terms in square brackets can be interpreted as a electron conversion from the X valley of AlAs to the Γ valley of GaAs followed by the elecron-hole recombination; they are small, since $t_{13}^z \ll 1$. The second ones are due to indirect electron-hole recombination;[12] they occur only at the interface and, therefore, have a small factor $a/d_{1,2}$. This factor is not so small in short-period superlattices where $d_{1,2}$ are as large as a few lattice constants. The indirect electron-hole recombination prevails in such structures, if $a/d_{1,2} \gg t_{13}^z$. We omit the terms that contain both these factors or $|1-t_{44}^z| \ll 1$.

The question arises, how small should be $|\mathcal{P}_1|$ in order to Eq. (1) holds? This is possible if the deviation of $|\mathcal{P}_2|^2$ from its average value in Eq. (10) essentially exceeds $|\mathcal{P}_1\mathcal{P}_2^*|$, i.e., when $|\mathcal{P}_1|^2 \ll (h/l)^2|\mathcal{P}_2|^2$ or

$$\frac{\overline{w}^2}{\sigma^2} \ll \frac{h^2}{l^2}. \tag{15}$$

III. KINETICS OF EXCITON LUMINESCENCE IN TYPE-II GaAs/AlAs SUPERLATTICES. EXPERIMENT

The undoped GaAs/AlAs type-II superlattices used in this study were grown by molecular-beam-epitaxy at 600^oC on a (100) GaAs substrate. The sample BP205, where the X_z excitons were studied, contains 40 periods of 19.8-$\mathring{A}$ GaAs/25.5-$\mathring{A}$ AlAs. The X_{xy} excitons were studied in the sample BP354. It contains 25 periods of 25-$\mathring{A}$ GaAs/83.5-$\mathring{A}$ AlAs.

The time-resolved photoluminescence of X_z excitons was excited by a YAG:Nd pulse laser with wavelength $532\,nm$, the pulse duration was $0.15\,\mu s$. The N_2 laser with wavelength $337\,nm$ and pulse duration $7\,ns$ was used to investigate the time-resolved photoluminescence of X_{xy} excitons.

The luminescence was analyzed by a double grating monochromator equipped with a photomultiplier. Lifetime measurements were made by the time correlated single-photon counting technique. The samples were immersed in liquid helium.

Figures 2 and 3 present the experimental results on the exciton decay rates in our samples. Theoretical curves was derived from Eqs. (1), (12). The values of parameters $w_0 = 320\,c^{-1}$, $w_r = 0.002 \times 10^6\,c^{-1}$, $\overline{w} = 0.1 \times 10^6\,c^{-1}$, and $\sigma = 0.61 \times 10^6\,c^{-1}$ ensure the best fit with the experiment. We see that Eq. (1) fits the experimental data for the decay rates of X_{xy} excitons in the sample BP354, whereas Eq. (12) is more appropriate for X_z excitons in the sample BP205. Note that the value of w_0, which is associated with the phonon-assisted recombination, is small in both curves. That is really the case at a low temperature. Recombination of X_{xy} excitons is considerably slower than that of X_z excitons. This means that the interfaces in our samples are perfect enough to apply our theory for interpretation of the experimental data.

Expressions (11) – (14) allow to estimate the function $\tilde{W}(k)$ at the points $k = 0$ and $k = 2\pi/a$. This is not sufficient to determine the function. However, it is possible to estimate the parameters of the rough interface if we restrict ourself to the particular type of the correlation function. We assume the exponential correlation function

$$W(\rho) = h^2 \exp(-\rho/l), \tag{16}$$

where l is the correlation length. This type of the correlation function is more appropriate to our model of the rough interface (Fig. 1); it allows to construct the two-position distribution, so that the distribution of slopes has a δ-singularity, i.e., the slope is always zero exept a set of points (like point 1) with measure zero.[13] This is impossible for the Gaussian correlation function $W(\rho) = h^2 \exp(-\rho^2/l^2)$ most frequently employed in theoretical discussions.[14] Fourier transform of the exponential function is

$$\tilde{W}(k) = \frac{2\pi h^2 l^2}{(1 + k^2 l^2)^{3/2}}. \tag{17}$$

Unlike the Gaussian function it has not exponential factor, which is small at a large k. This is also due to the singular points 1; only in the vicinity of these points the momentum relaxation of indirect X_{xy} excitons is possible.

If we assume that correlation functions are equal for the interfaces of both our samples, then substitution of Eq. (17) into Eqs. (11) and (14) allows to find the values of h and l.

The decay parameters of the wave functions $\gamma_{X_z,X_{xy},h}$ in these expressions are determined by Eq. (7) for the known energies of the electrons or holes. As regards to $U_{\Gamma,X}$, these values can be estimated only from the band structure calculations for GaAs and AlAs. However, the first terms in the expression for $\overline{w}$ and σ^2 (14) can be omitted. Indeed, $t^z_{13} = t_{\Gamma X} m_\Gamma^{\mathrm{GaAs}}/(m_e a \gamma^r) < 0.06$, whereas $a/d_1 = 2/7$, i.e., the indirect recombination of X_z exitons at the interface prevails in our samples. Then the values of $\sigma^2/\overline{w}^2$ and $w_r/\overline{w}$, which are determined from experimental data, become independent of $U_{\Gamma,X}$. For our experiments this estimation yields

$$\frac{\sigma^2}{\overline{w}^2} = \frac{1}{2}\left(\frac{2\pi}{a}\right)^2 \left(\frac{\gamma_h}{\gamma_{X_z} d_2} - \frac{1-t^h_{22}}{t^h_{22} d_1}\right)^2 \tilde{W}(0),$$

$$\frac{w_r}{\overline{w}} = \frac{4\pi^4 \gamma_h^2 {t^h_{22}}^2 {d_1^{X_{xy}}}^3 d_2^{X_{xy}}}{a^4 {d_1^{X_z}}^3 {d_2^{X_z}}^3} \left[\frac{(1-t^h_{22})^2}{\tilde{\gamma}^4_{X_{xy}}} + \frac{(1-t^{xy}_{22})^2}{\tilde{\gamma}^4_h}\right] \tilde{W}\left(\frac{2\pi}{a}\right). \tag{18}$$

Here $d_1^{X_z}$, $d_2^{X_z}$, $d_1^{X_{xy}}$, and $d_2^{X_{xy}}$ are widths of GaAs and AlAs layers in the samples BP205 ($d_1^{X_z}$, $d_2^{X_z}$) and BP354 ($d_1^{X_{xy}}$, $d_2^{X_{xy}}$) where X_z and X_{xy} excitons were studied;

$$\gamma_{X_z} = \frac{1}{\hbar}\sqrt{2m_{Xl}^{GaAs}\left[E_X^{GaAs} - E_X^{AlAs} - \frac{\hbar^2}{2m_{Xl}^{AlAs}(d_2^{X_z})^2}\right]},$$

$$\gamma_h = \frac{1}{\hbar}\sqrt{2m_{hh}^{AlAs}\left[E_h^{GaAs} - E_h^{AlAs} - \frac{\hbar^2}{2m_{hh}^{GaAs}(d_1^{X_z})^2}\right]}, \quad t^h_{22} = \frac{m_{hh}^{AlAs}}{m_{hh}^{GaAs}},$$

$$\tilde{\gamma}_{X_{xy}} = \frac{1}{\hbar}\sqrt{2m_{Xt}^{GaAs}\left[E_X^{GaAs} - E_X^{AlAs} - \frac{\hbar^2}{2m_{Xt}^{AlAs}(d_2^{X_{xy}})^2}\right]}, \quad t^{xy}_{22} = \frac{m_{Xt}^{AlAs}}{m_{Xt}^{GaAs}},$$

$$\tilde{\gamma}_h = \frac{1}{\hbar}\sqrt{2m_{hh}^{AlAs}\left[E_h^{GaAs} - E_h^{AlAs} - \frac{\hbar^2}{2m_{hh}^{GaAs}(d_1^{X_{xy}})^2}\right]}, \quad \gamma^r = \frac{1}{\hbar}\sqrt{2m_\Gamma^{AlAs}\left(E_\Gamma^{AlAs} - E_X^{AlAs}\right)};$$

$E_{\Gamma,X,h}^{GaAs,AlAs}$ are positions of the band extrema in GaAs and AlAs, m_Γ^{GaAs} is effective mass of Γ valley of GaAs, $m_{Xl,Xt}^{GaAs,AlAs}$ are longitudial and transversal effective masses in X valleys of GaAs and AlAs, $m_{hh}^{GaAs,AlAs}$ are effective masses of heavy holes in GaAs and AlAs, and m_e is mass of a free electron. We assume $t^h_{21} \ll \gamma_h \sim 2/a$; this is the result of calculations.[7]

Eq. (18) estimates the values of For the height h and diameter L [$L = 4l$ for the distribution (16)][13] of the roughnesses we find $h \approx 1.25a$ and $L \approx 9a$. This is in agreement with structural reseach of the GaAs/AlAs interface where the steps with the height $h = a/2$ and the mean length of 40–200 Å were observed (see Ref.[9] for the review).

Rough estimation of h and l values also can be done if we assume that criterium (15) holds. This justifies Eq. (1) for X_z excitons where $w_0 \equiv w_0^{X_z} = \Lambda|\mathcal{P}_1|^2$ and $w_r \equiv w_r^{X_z} = \Lambda|\mathcal{P}_2|^2$. Using Eq. (13), we find the expressions for $2w_r^{X_z}/w_0^{X_z}$ and $w_r/w_0^{X_z}$ [unlike $w_r^{X_z}$ the w_r value correspondes to X_{xy} excitons (Fig. 3) and determined by Eq. (11)]. These expressions accept the form of Eq. (18) after the substitutions $\sigma^2/\overline{w}^2 \to 2w_r^{X_z}/w_0^{X_z}$ and $w_r/\overline{w} \to w_r/w_0^{X_z}$ of their left sides. The values of $w_0^{X_z} = 0.11 \times 10^6\, c^{-1}$ and $w_r^{X_z} = 0.38 \times 10^6\, c^{-1}$ ensure the best fit of the dashed line (Fig. 2) with experiment. This estimation yields $h = a$, $L = 8.8a$, which are close to the values obtained from Eq. (12). For this reason both theoretical curves (Fig. 2) fit experimental data at small times. Nevertheless, Eq. (12) better fits the experimental data at large times where it unsure the slower decay of the luminescence: $I(t) \propto \exp(-\overline{w}t)/t$, instead of $I(t) \propto \exp(-w_0 t)/t^{3/2}$ as it is predicted by Eq. (1).

IV. DISCUSSION

In this paper we investigate the exciton luminescence in type II GaAs/AlAs superlattices. We use the envelope function approximation to consider the exciton recombination at an interface. To justify this approach, we have to note that envelope function approximation has been used only to find the reflection and transmission coefficients. While the Bloch functions f_e and f_h has been used to find the probability of the exciton recombination. The error arises only when we consider the Bloch amplidudes $u_\Gamma(\mathbf{r})$, $u_X(\mathbf{r})$, and $v(\mathbf{r})$ as periodical functions at the interface. Indeed, the deviation of these amplitudes from their bulk values arises only at a small distance from the interface; this deviation is especially small for the contacts of similar materials (e.g., GaAs/AlAs).[7,15]

It seems the boundary conditions (4) connect a very few valleys of the electron spectrum to consider the interface influence on the exciton recombination; nevertheless, it is not the case. Indeed, the electron wave functions in the valleys that are not explicitly involved in Eq. (4) are strongly localized at the interface. This allows to consider them in terms of the boundary conditions where the parameters t_{ik} are influenced by these valleys. This procedure had been described when Eq. (4) was derived. The error arises only when these parameters are considered as independent of the electron energy; that is possible if the energy difference between the bottoms of the appropriate valleys considerably exceeds the exciton energy. Note that a lot (about 10) of the electron bands are sometimes taken into account when the parameters of the interface matrix are calculated.[17]

We use the boundary conditions for the envelope wave function to consider $\Gamma - X$ mixing of electrons at the interface. This approach is more general than the kinetic model proposed in Ref.[16]. The kinetic equation where the electron states in the Γ and X valleys are considered as independent can be used for low $\Gamma - X$ mixing. Only in that case it is possible to add the probabilities for the electron to be in Γ and X valleys. It should be noted that we also assume the small value of $\Gamma - X$ mixing ($|t_{13}^z| \ll 1$). However, this approximation is not principal for our consideration; it only makes the results [Eqs. (7), (11), (14), and (18)] not so cumbersome.

Influence of a nonstochastic process on the exciton recombination in Ref.[1] is considered by the exponential factor $e^{-w_0 t}$. This factor could be obtained if we insert the corresponding term in τ-approximation into the kinetic equation for the exciton density. If the τ-approximation is not applicable for the process, then this factor becomes nonexponential.[3] Correlation between stochastic and nonstochastic processes changes the second factor in Eq. (1). In this case the probability of the exciton recombination w is not a simple sum of the probabilities of each process. As the result, the additional terms arise in the expression for w [the second and third terms in Eq. (10)]. These terms are linear in the stochastic variable, so that their averages vanish. For this reason they are not important when the mean intensity of the luminescence or the light absorption[6] is considered. However, they are important for the kinetic phenomena, because they determine the mean square of the deviation σ of the stochastic variable from its mean value. The nonexponential behavior of the decay rate Eq. (12) valids any time when linear with respect to the stochastic variable terms are main in the expression for w. Such a situation can occur also in other type-II semiconductor structures where the interface influence is essential, e.g., in quantum dots.[18]

Expressions (11) and (14) relate parameters of the radiative decay rates ($w_r, \overline{w}$, and σ) with the correlation function of the rough interface. The values of the Fourier transform of this function at two particular points, $k = 0$ and $k = 2\pi/a$, are necessary for these relations. This allows to estimate the parameters only for simplest functions [like Eq. 16]. The real interface might be more complicated. In particular, a few different scales could be characteristic for the roughnesses at the interface. Expressions (11) and (14) takes into account all these factors; however, it is impossible to determine more than two parameters from the time-resolved luminescence experiments only.

Comparing the experimental results (Figs. 2 and 3), we see that mean lifetime of X_{xy} excitons essentially exceeds that of X_z excitons. This happens due to recombination of X_z excitons at a plane interface. Meanwhile, influence of the roughnesses, i.e., the nonexponential factor in $I(t)$, is more essential for X_z excitons. This can be understood from our analysis. Indeed, $\sigma \propto \tilde{W}(0)$, whereas $w_r \propto \tilde{W}(2\pi/a)$ while $\tilde{W}(2\pi/a) \ll \tilde{W}(0)$. The recombination occurs in some region near the step (point 1 in Fig. 1). The size of this region is of the order of $|\mathbf{q}_\|\|^{-1}$, where $\mathbf{q}_\|$ is the parallel-to-interface component of the electron wave vector. This region is large for X_z electrons ($|\mathbf{q}_\|| \simeq r_B^{-1}$, where r_B is the exciton radius) but it is small for X_{xy} electrons ($|\mathbf{q}_\|| \simeq 2\pi/a$). As the result, the small factor [of the order of $(a/l)^3$] arises in the expression for w_r.

In conclusion, kinetics of the exciton luminescence at a rough interface has been considered. The Klein *at al.* law (1) is shown to be valid for the decay rate of X_{xy} excitons, whereas the more complicated expression (12) is applicable for X_z excitons. Expressions (11) and (14), which relate the parameters of the exciton kinetics with statistical characteristics of the rough interface, allow to estimate some of these characteristics from the experimenal data. The values of the mean height $7\,\mathring{A}$ and length $50\,\mathring{A}$ of the roughnesses obtained from our experiments are in a good agreement with the results of structural investigations of the GaAs/AlAs interface.

ACKNOWLEDGMENTS

Authors wish to thank Prof. E. L. Ivchenko for valuable discussions. This work was supported by the Russian Foundation for the Basic Research, Grants No. 99-02-17019, 98-02-17896, 00-02-17658, and the Program "Physics of Solid State Nanostructures" by the Russian Interdisciplinary Scintific and Technical Council, Grant No. 99-1133.

REFERENCES

[1] M. V. Klein, M. D. Sturge, and E. Cohen, Phys. Rev. B, **25**, 4331 (1982).

[2] F. Minami *et al.*, Phys. Rev. B, **36**, 2875 (1987).

[3] I. N. Krivorotov *et al.*, Phys. Rev. B, **58**, 10687 (1998).

[4] S. Nagao *et al.*, J. of Crystal Growth, **175**, 10687 (1997); B. A. Wilson *et al.*, Phys. Rev. B, **40**, 1825 (1989); E. Finkman *et al.*, J. Lumin. **39**, 57 (1987); B. A. Wilson *et al.*, J. Vac. Sci. Technol. B **6**, 1156 (1988).

[5] E. L. Ivchenko and G. E. Pikus, *Superlattices and Other Heterostructures. Symmetry and Optical Phenomena*, second ed. (Springer-Verlag, Berlin, 1997).

[6] L. Braginsky, Physica E, **5**, 142 (1999).

[7] T. Ando and H. Akera, Phys. Rev. B, **40**, 11619 (1989).

[8] D. Lüerßen *et al.*, Phys. Rev. B, **59**, 15862 (1999).

[9] F. Bechstedt, R. Enderlein, *Semiconductor Surfaces and Interfaces. Their Atomic and Electronic Structures*, (Berlin: Akademie-Verlag, 1988).

[10] I. L. Aleiner and E. L. Ivchenko, Fiz. Tech. Poluprovodn. **27** 594 (1993) [Sov. Phys. Semicond. **27** (1993)]; Y. Fu, M. Willander, E. L. Ivchenko, and A. A. Kiselev, Phys. Rev. B, **47** 13498 (1993).

[11] F. G. Bass and I. M. Fuks, *Wave Scattering from Statistically Rough Surfaces*, (Pergamon Press, 1979).

[12] L. Braginsky, Phys. Rev. B, **57**, R6870 (1998).

[13] M. V. Berry, Phil. Trans. **A273**, 611 (1973); J. M. Ziman, *Models of Disorder. The theoretical physics of homogeneously disordered systems*, (Cambrige University Press, 1979).

[14] For the exciton problem this approximation has been used in V. A. Kosobukin, Fiz. Tverd. Tela **41**, 330 (1999) [Phys. of Solid States **41**, XXX (1999)]; see also the references therein.

[15] P. von Allmen, Phys. Rev. B, **46**, 15377 (1992).

[16] M. Maaref *et al.*, Solid State Commun., **81**, 35 (1992).

[17] S. N. Grinyaev, private communication; see, e.g., S. N. Grinyaev and G. F. Karavaev, Fiz. Tverd. Tela **42**, 752 (2000) [Phys. of Solid States **42**, XXX (2000)].

[18] A. O. Govorov and A. V. Chaplik, Sov. Phys. JETP 72, 1037 (1991) [Zh. Eks. Teor. Fiz. 99, 1853 (1991)]; A. V. Kalameitsev, A. O. Govorov, and V. Kovalev, JETP Lett. 68, 669 (1998) [Pis'ma Zh. Eks. Teor. Fiz. 68, 634 (1998)].

FIGURES

FIG. 1. The model of the rough interface: side view.

FIG. 2. Temporal evolution of the X_z exciton emmision. Theoretical curves (dashed and solid lines) was derived from Eqs. (1) and (12) respectively. Dotts show the experimental data.

FIG. 3. Temporal evolution of the X_{xy} exciton emmision. Theoretical curve (solid line) was derived from Eq. (1). Dotts show the experimental data.

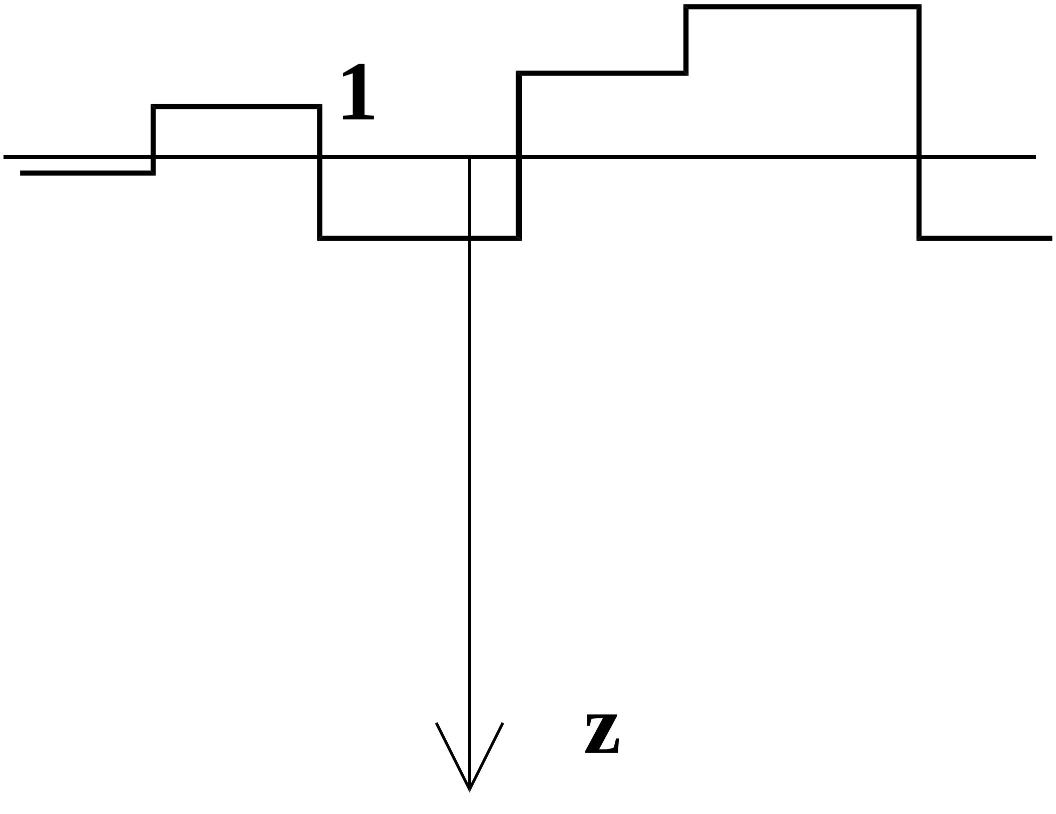
1
z

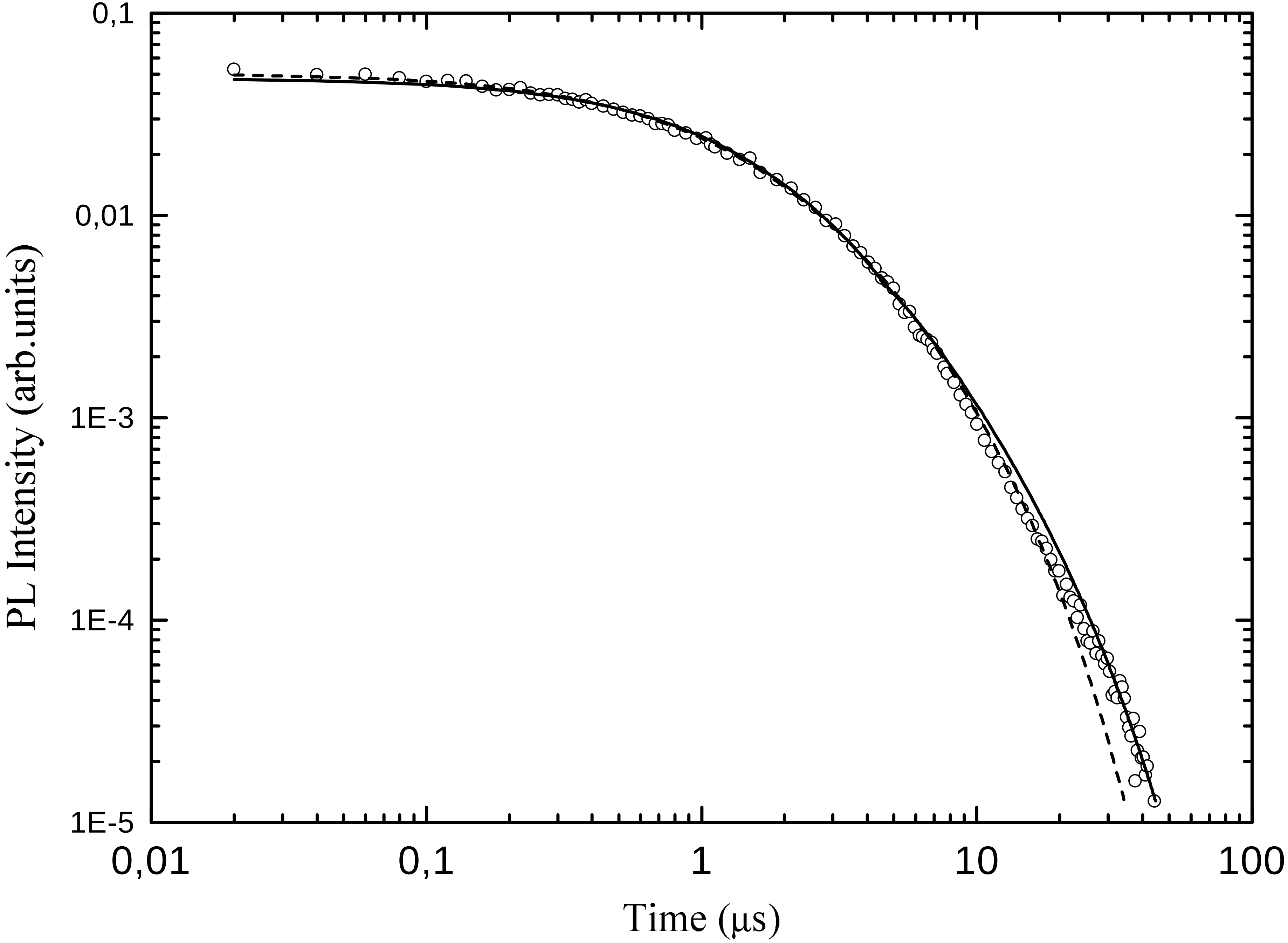
0,1
0,01
1E-3
1E-4
1E-5
0,01
0,1
1
10
100
PL Intensity (arb.units)
Time (µs)

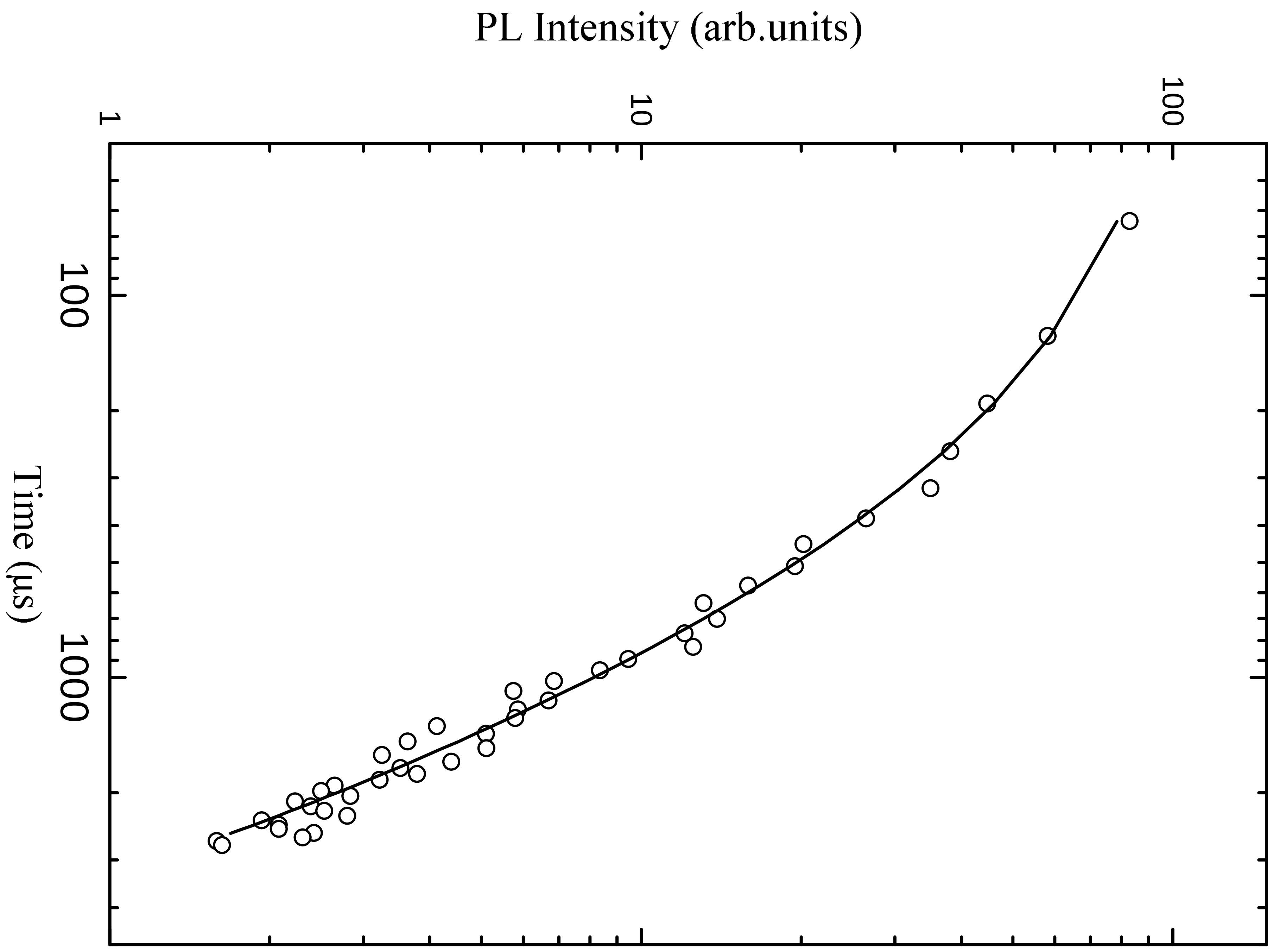
PL Intensity (arb.units)
1
10
100
Time (μs)
100
1000